FIBRE ORIENTATION STRUCTURES AND THEIR EFFECT ON THE CRACK RESISTANCE OF AN INJECTION MOULDED TRANSVERSE RIBBED PLATE

P.J.Hine*, R.A.Duckett*, P.Caton-Rose# and P.D.Coates#

* - IRC in Polymer Science and Technology, Physics Department, University of Leeds, Leeds LS2 9JT
# - IRC in Polymer Science and Technology, University of Bradford, Bradford.

ABSTRACT

In this paper we describe an extensive study of the fibre orientation structures developed in a transverse ribbed plate during injection moulding, and the use of these structures to investigate the effect of the local fibre orientation state on crack initiation resistance. The fibre orientation results for the ribbed plate, measured using large area image analysis system developed at Leeds University, showed that after an initial settling down period, the central core region, where the fibres are aligned perpendicular to the flow direction, decreased in size monotonically, with an associated monotonic increase in the outer shell regions, where the fibres are aligned preferentially along the injection direction. Interestingly, the level of orientation in the two regions remained almost constant: only the proportions of the two regions were found to change with flow length. Across the plate, close to the gate, the central core region was found to have a lens like shape, while at the other end of the plate the core was thinner and also consistent in thickness across the sample width. The transverse rib was found to cause little disturbance to the fibre orientation of the base plate.
The different proportions of the shell and core regions at different locations over the ribbed plate provided an ideal opportunity to test the proposition of Friedrich that the crack resistance of a short fibre reinforced material depends on the number of fibres that are perpendicular to the crack tip. The impact test results gathered in this way confirmed this hypothesis of Friedrich.

INTRODUCTION

For many years thermoplastics have been extensively used in a wide variety of applications because they are relatively cheap, inert and are easy to manufacture into component shapes, particularly by injection moulding. However, commodity polymers, such as polypropylene and Nylon, have relatively poor mechanical properties which limits their use to non-structural applications at modest temperatures. Short glass fibre reinforcement is well established as a means of significantly improving on mechanical performance without compromising processability, and many glass filled polymer grades and products are commercially available. Apart from the fibre and matrix properties, the mechanical properties of the final component are crucially dependent on the fibre orientation distribution developed during the process, as well as other aspects such as the resulting fibre aspect ratio and the fibre/matrix interface. While the links between fibre orientation and mechanical properties are now well established [1, 2], strength and fracture predictions are less mature. The aim of this paper is to test the proposal of Friedrich [3] that the crack resistance of a short fibre reinforced material depends on the number of fibres that are perpendicular to the crack tip.

EXPERIMENTAL

The model component examined in this study was a rectangular plate, with a single transverse rib placed 38mm from the gate: the rib was 3mm thick at the root, 2mm at the tip and 12mm high (Figure 1). The material used in this study, kindly supplied by Birkbys Plastics Ltd, was Rhodia Technyl Grade C216 V40: a 40w/w glass fibre reinforced nylon 6.

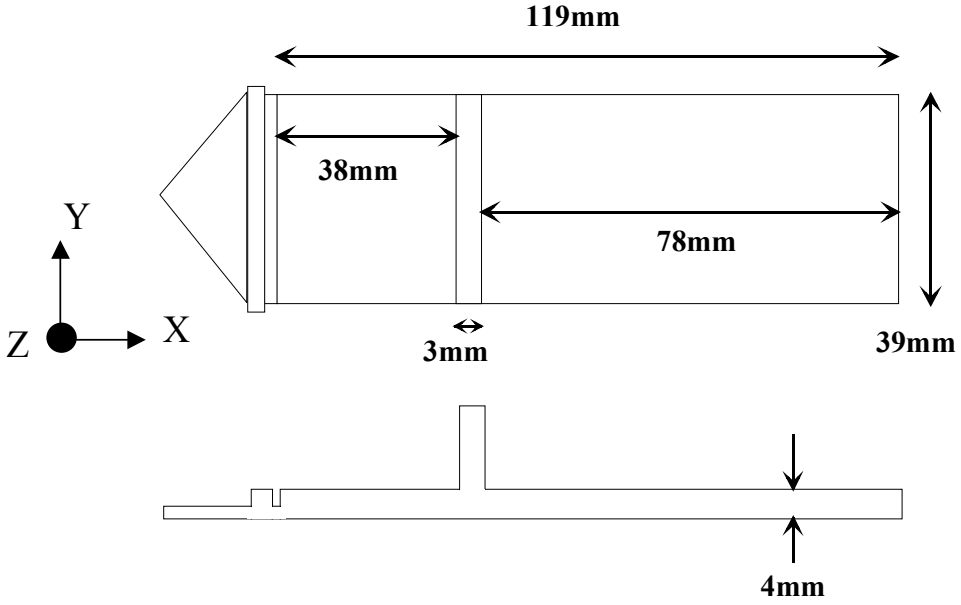

Figure 1: Details of the transverse ribbed plate

The transverse ribbed plate under study here has already formed part of a previous joint Leeds/Bradford PhD programme [4], making it an ideal choice for the expanded work to be undertaken here. As the former work had concentrated on the fibre orientation structures around the rib root area, a clear target for the current study was to investigate the fibre orientation over the whole component.

Measurement of fibre orientation was carried out using an in-house developed 2D image analysis system developed at Leeds. This system relies on the fact a cylindrical fibre makes an elliptical footprint where it meets the surface of a 2D section (a typical section is shown in Figure 2a). Measuring the ellipticity of each fibre image allows the two angles θ and ϕ, that specify the 3D spatial orientation of each fibre, to be obtained (Figure 2b). Sections are accurately taken from the chosen position using a Struers Accutom-5 cutting machine, potted in epoxy resin, polished to give an optically flat surface and then etched in an oxygen plasma to give contract between the fibre and matrix phases. The image frame shown in Figure 2a, viewed in reflected light at a typical scanning magnification of 500, has been prepared in such a manner. The recent implementation of a Windows based system now allows areas of up to 30mm x 30mm to be accurately and quickly scanned, which can incorporate up to a million fibre images. This allows areas of cm^2 to be analysed in detail, which is of the appropriate size over which mechanical properties are usually measured.

A full description of the image analysis technique, and the various post-processing routines used for analysing the data, can be found in [5, 6]

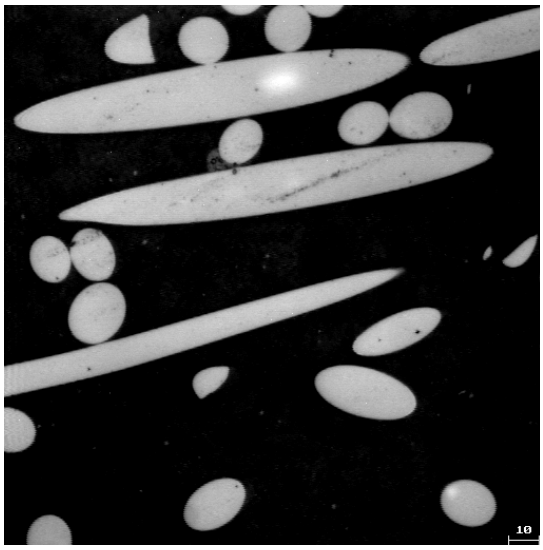

Figure 2a: Typical image analysis frame

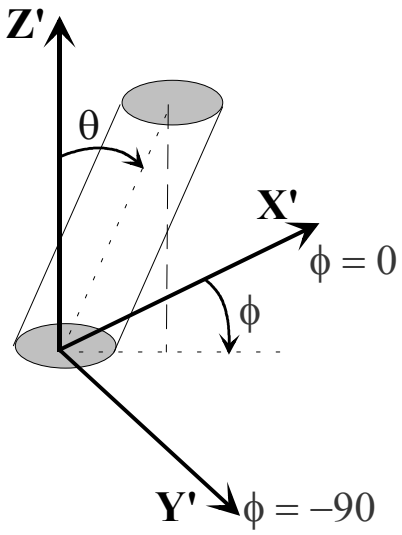

Figure 2b: Definition of θ and ϕ

For carrying out the fracture measurements, three point bend samples were cut from the injection moulded plates at positions chosen following the characterisation of the fibre orientation. These samples were tested at an impact speed of 1 m/s using a ROSAND instrumented falling weight impacted tester Type 5. All the fracture samples were conditioned for 3 days in a cell containing a water/Calcium nitrate mixture to give an atmosphere of 50%RH. Following a previous study by one of the authors [7] samples were cut to allow the initial crack tip to be placed either parallel to the injection direction (longitudinal or L samples) or perpendicular to the injection direction (transverse or T samples) as shown schematically in Figure 3: for the L and T samples the crack is placed across the sample and so 'sees' an average of the through-thickness orientation. In addition, a few samples were prepared with through thickness cracks (designated TT as shown in Figure 3) where the crack tip is placed at a particular position within the sample thickness.

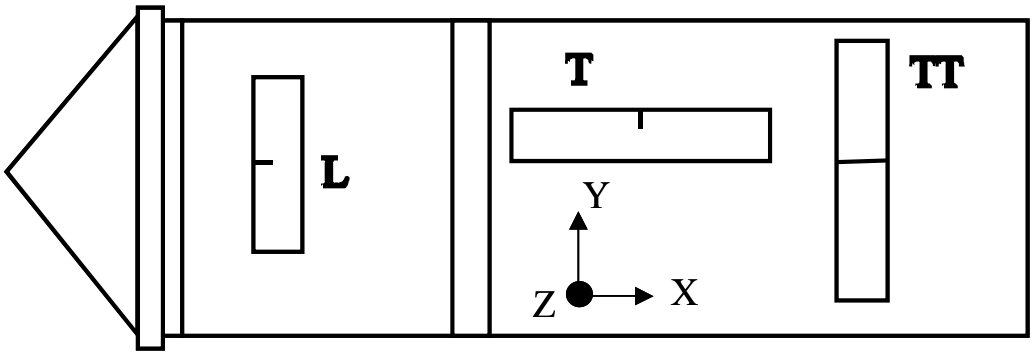

Figure 3: Definition of the longitudinal [L], transverse [T] and through thickness [TT] fracture samples.

Samples were tested under the ESIS protocol [8] using a nominal crack length to sample width ratio of 0.5 and a bending span to sample width ratio of 4: the crack tip was introduced using a shaping machine.

THEORY

The central idea postulated by Friedrich [3] for crack propagation in a short fibre reinforced composite is that fibres that are perpendicular to the crack tip are much more effective at absorbing energy (as they have to be pulled out of their sockets or broken) compared to fibres that are parallel to the crack tip, whereby fracture can proceed through the polymer matrix phase without significantly disturbing the fibres.
Friedrich proposed an empirical non-linear orientation function, f_{peff}, to capture the form of this behaviour

$$f_{peff} = \alpha\left[1 + \tanh\left(\beta f_p\right)\right], \qquad \alpha = 0.5, \beta \text{ from } 0...5 \qquad (1)$$

$$\text{and } f_p = \left(1 - 2 < \cos^2 \theta_{perp} >\right) \qquad (2)$$

where $<\cos^2\theta_{perp}>$ is the average value of the second order orientation average with respect to the crack propagation direction (i.e, when $<\cos^2\theta_{perp}>=0$ all fibres lie perpendicular to the crack direction and f_p =1 and f_{peff} = 1).
In this work we use a similar form for f_{peff}, but redefine q with respect to the crack plane normal. Now f_p =1 and f_{peff} = 1 when the all fibres are aligned perpendicular to the crack tip direction and the form of f_p becomes

$$f_p = \left(2 < \cos^2 \theta_{crackplanenormal} > -1\right) \qquad (3)$$

Friedrich also proposed that the strain energy release rate G_c, or the energy to initiate a crack in the material, takes the following form:

$$G_c = A f_{peff} + B \qquad (4)$$

where A accounts for the energy absorbing processes due to the fibres (pull out etc) and B the energy absorbing process due to the matrix: here f_{peff} would be an average fibre orientation across the sample thickness at the crack tip.

RESULTS

In the first series of measurements, YZ sections were taken parallel to the Y axis at two distances from the gate, 16.5mm and 67mm (which is 25mm from the back of the rib): these two sections are designated a and b respectively (Figure 4). With fibre orientation distribution (FOD) data there are many of ways of presenting the results. One method which we find useful, is to display the measured FOD in terms of maps of the average values of the principal second order orientation tensors $<\cos^2\theta_X>$, $<\cos^2\theta_Y>$ and $<\cos^2\theta_Z>$, also known as a_{XX}, a_{YY} and a_{ZZ}.. These parameters, which were first proposed by Advani and Tucker as a useful way of describing orientation data [9] are equal to 1 for perfect alignment with respect to a particular axis, equal to 0 when aligned perpendicular to that axis and all three parameters add up to one. In regions where the orientation is predominantly planar, as it is in the plate regions of the ribbed component, then only one parameter, $<\cos^2\theta_X>$, is required ($<\cos^2\theta_Z>\sim 0$, and $<\cos^2\theta_Y> \sim [1- <\cos^2\theta_X>]$). Figure 4 shows two maps of the value of $<\cos^2\theta_X>$ at position a and position b. Here white indicates a value of 1 (perfect alignment along the X axis or the injection direction) and black a value of 0 (perfect alignment in the Y axis or perpendicular to the injection direction in the plane of the plate).It is seen that near the gate (position a) there is a centrally located lens shaped ‘core’ region where the fibres are preferentially aligned perpendicular to the injection direction (i.e. black), and outer ‘shell’ regions where they are aligned parallel to the injection direction. Farther from the gate (position b), the core is much thinner and is a uniform thickness across the sample.

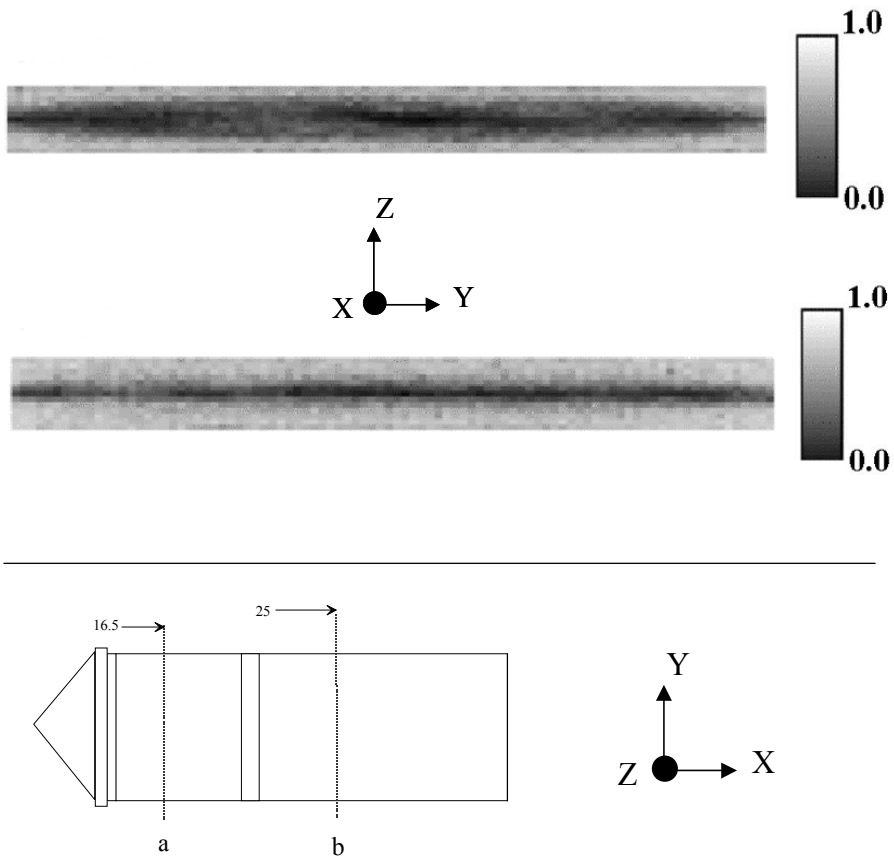

Figure 4: Area maps of the second order orientation tensor <cos2θX> for YZ sections at positions a and b.

The FOD was also measured along the centre line of the sample as shown in Figures 5 and 6. The length of the sample was split into three, not quite overlapping, sections of ~35mm in length. Section c was taken between the gate and the rib and sections d and e after the rib. Directly after the gate, and at the far end of the plate, the orientation is close to random ($\langle\cos^2\theta_X\rangle = \langle\cos^2\theta_Y\rangle = \langle\cos^2\theta_Z\rangle \sim 1/3$). Away from the gate there is a settling down period of distance of ~ 10mm after which the average orientation across the sample thickness changes monotonically until a similar distance from the sample end. In this region the value of $\langle\cos 2\theta_X\rangle$ increases monotonically and the value of $\langle\cos^2\theta_Y\rangle$ similarly decreases: the out-of-plane orientation in this central section $\langle\cos^2\theta_Z\rangle$ is almost zero ($\langle\cos^2\theta_Z\rangle \sim 0.04 \pm 0.01$). The presence of the rib (at~38mm from the gate) has little effect on the overall FOD pattern in the plate.

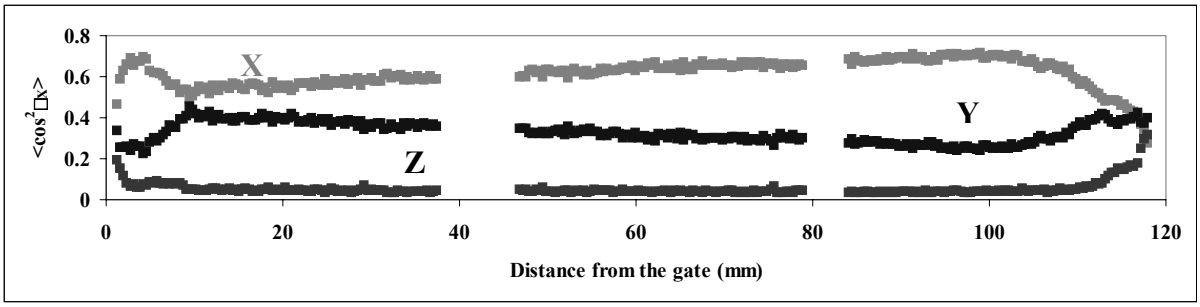

Figure 5: Values of the second order orientation tensors along the length of the sample (averaged in strips parallel to the Z axis)

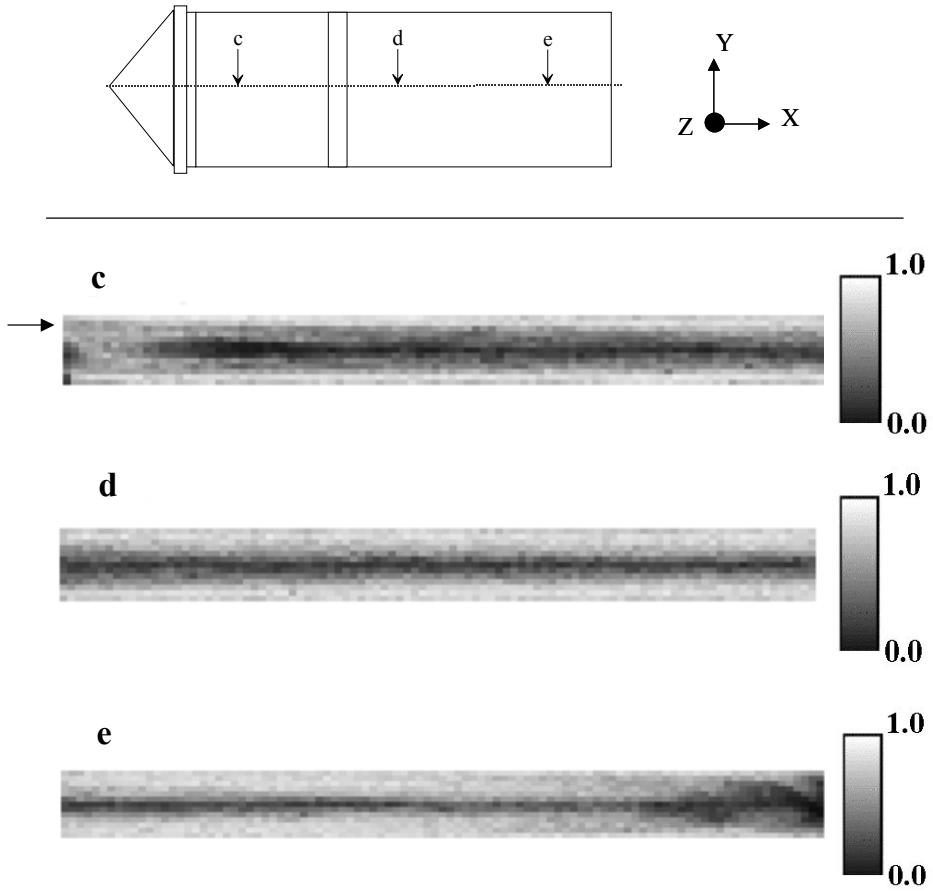

Figure 6: Area maps of the second order orientation tensor $\langle \cos^2\theta_X \rangle$ along the centre line for positions a, b and c

The results in Figures 5 and 6 confirm the overall increase in X orientation with distance from the gate as already indicated from the analysis of the transverse sections a and b. Figure 7 shows the calculated percentage of the core and shell regions with distance from the gate: the two shell regions symmetrically on either side of the core were found to increase in size at the expense of the core. Figure 8 shows the level of orientation in the two regions, and it is seen that the value of orientation is approximately constant, demonstrating that the increase in average through thickness X orientation indicated in Figure 5 is due to an increase in the thickness of the shell region, rather than an increase in the preferred orientation in the shell layers.

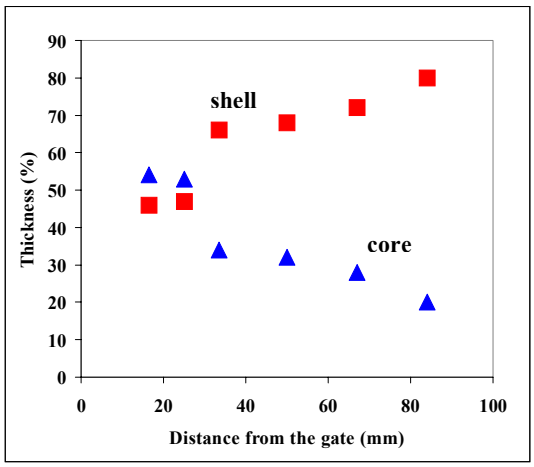

Figure 7: Shell and core sizes

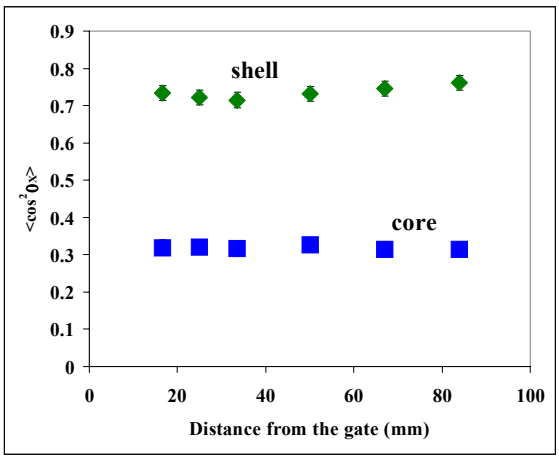

Figure 8: Orientation in the shell and core

The different orientation structures characterised within the transverse ribbed plate present an ideal opportunity for investigating the effects of local fibre orientation structures on impact fracture toughness. By testing samples at different locations and by sending crack in different directions, a range of orientation states at the crack tip can be achieved allowing the proposed relationship of Friedrich to be tested. T crack samples were cut at positions a and b and L crack samples were cut at 25, 50, 67 and 84 mm from the gate to match up with image analysis measurements at the same positions. In addition, through thickness samples (TT) were cut with the centre of the crack tip 84mm from the gate. This crack was placed at a depth ratio of 0.2 so that the crack tip was located in the shell region of the plate. In all cases the crack tip was positioned at the same point as (or as close as possible to) that measured by image analysis.

Figure 9 and 10 shows typical fractures surfaces for T crack sample taken at positions a and b. The different shell/core ratios at the two positions are clearly seen in these pictures in terms of surface appearance.

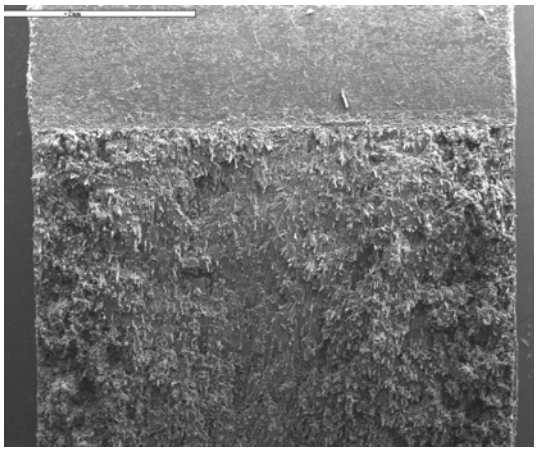

Figure 9: T crack – position a.

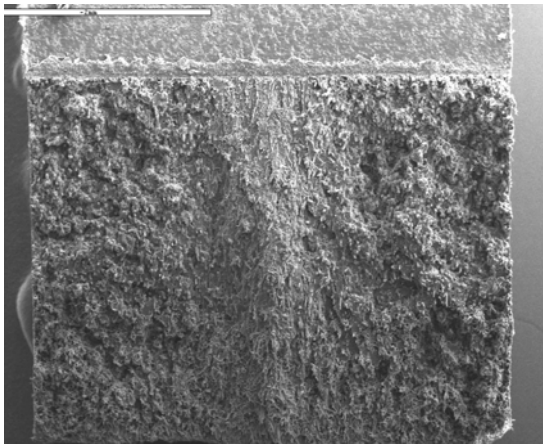

Figure 10: T crack position b

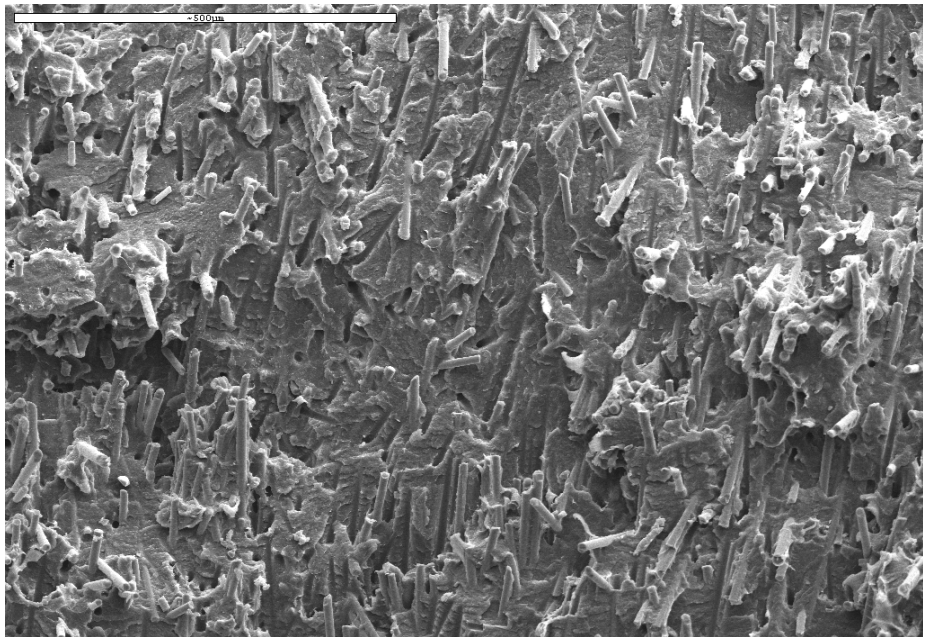

Figure 11: Higher magnification picture of core region in Figure 9.

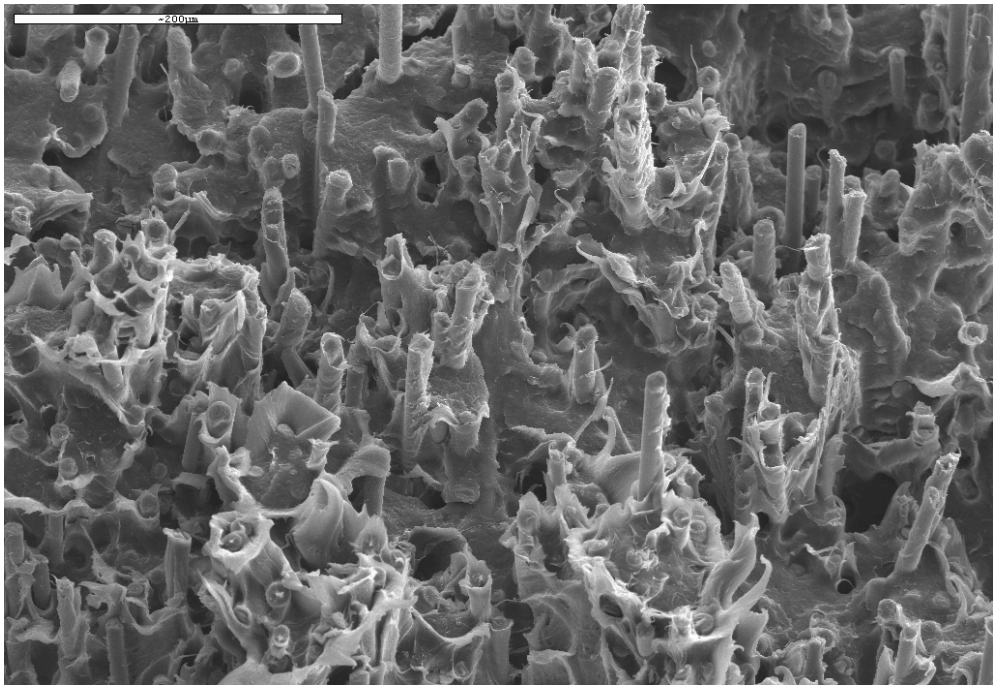

Figure 12: Higher magnification picture from the shell region in Figure 10.

Figure 11 shows the central core region at position a. As expected, the fibres here, being parallel to the crack propagation direction, lie in the plane of the crack plane: there is little evidence of ductility in the matrix and it would be expected that only a small amount of energy would be absorbed for crack propagation in this region. Conversely, Figure 12 shows a typical fracture surface in the shell region of position b where the fibres are perpendicular to the crack tip. Here there is evidence for a large number of the fibres having been pulled from out of the other surface, and associated empty sockets for fibres pulled out of this surface. In addition the matrix shows significant ductility both on and between the fibres. It is clear that this region will provide a significantly increased barrier to crack propagation. An important aspect is that the majority of the fibres have been pulled from the surface rather than broken, a mechanism which is thought to absorb more energy and suggests that the average fibre length is below the critical value for fracturing.

The critical aspect ratio for fibre breakage, S*, is given by [10]

$$S^* = \frac{\sigma_f^*}{2\tau^*} \qquad (5)$$

where σ_f^* is the fibre tensile strength and τ^* the critical interfacial shear strength. If we assume that it is the matrix surrounding each fibre that fails, we can equate τ^* to the shear yield strength of the matrix, τ_y. Putting the manufacturers values for σ_f^* and τ_y into equation 6 predicts a critical aspect ratio of ~ 44. As the average fibre aspect ratio was measured (by image analysis) to be 32, the presumption that the average fibre length is lower than the critical length appears valid.

Table 1 below shows the numerical results of the fracture tests carried out at the various positions across the transverse ribbed sample: at least three samples were tested at each position. Also shown is the average value of the second order orientation tensor parallel to the crack plane normal for each sample.

Fracture plane designation	Section details	G_c (kJ/m^2)	$\langle\cos^2\theta_{\text{plane normal}}\rangle$
L	25mm from the gate	11.2 ± 2.8	0.447
L	50mm from the gate	10.4 ± 1.5	0.363
L	67mm from the gate	8.05 ± 1.43	0.345
L	84mm from the gate	7.43 ± 1.28	0.295
T	position b	16.8 ± 1.4	0.603
T	position a	13.2 ± 0.5	0.491
TT	84mm from the gate	6.86 ± 0.60	0.245
TT	84mm from the gate	6.41 ± 0.30	0.210

Table 1: Fracture results at various positions across the transverse ribbed plate

It is seen that there is a clear correlation between the value of the fracture toughness and the level of orientation. The higher the value of $\langle\cos^2\theta_{\text{crack plane normal}}\rangle$, the greater the percentage of fibres that are transverse to the crack tip and the higher the value of the fracture toughness G_c. In order to cover as wide a range of crack tip orientation states as possible, a further sample was manufactured and tested, using the same fibre filled polymer. This component was a long thin bar (160mmlong x 10mm wide x 4mm thick) and the virtue of this geometry was that after moulding, the fibres were measured to be highly oriented along the bar axis ($\langle\cos^2\theta_{\text{axis}}\rangle$ = 0.86) and there was no core present so the orientation was homogeneous across the sample thickness. T crack samples were cut from this bar and fracture tests gave a value of G_c of 20.8 ± 1.5 kJ/m^2. This is consistent with the results in Table 6, as this latter sample showed the highest degree of orientation perpendicular to the crack tip and also the highest fracture toughness.

Figure 13 shows the fracture results plotted against the average crack tip orientation. Also shown on this graph is a solid line which represents the best fit to the Friedrich theory (equations 1,2 and 4). The graph shows that the proposed empirical theory does fit the measured behaviour very well. The value of α in equation 1 controls whether the relationship is symmetric about the endpoints: a

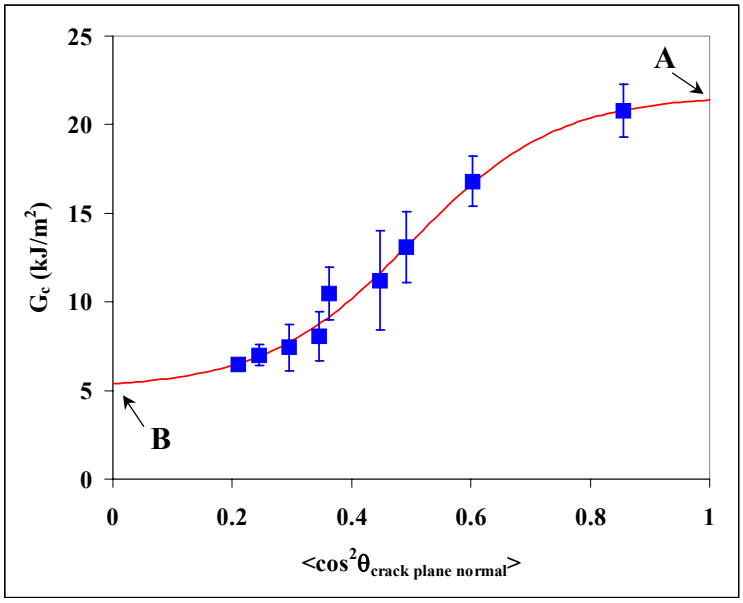

Figure 13: Measured strain energy release rate values at various average crack tip orientation values (■) and the best fit to the Friedrich theory (solid line)

value of ½ gives a symmetric shape. For the results shown on Figure 13, a floating fit of this parameter gave a value of 0.499, so we can safely consider this value as ½. We therefore have three independent parameters controlling the shape of the relationship: (A), – the fracture energy due to the fibres when all the fibre are perpendicular to the crack tip: (B) the fracture energy due to the matrix when all the fibres are parallel to the crack propagation direction: and β which controls how sharp the transition is between the endpoints. From the fitted data, for this polymer and this fibre volume fraction, the values obtained were A = 16.6 kJ/m^2, B = 5.1 kJ/m^2 and β = 2.1. Future work will be aimed at establishing whether these three parameters can be predicted from physical principles, which would then transform the empirical relationship into a predictive theory.

REFERENCES

1. Tucker III CL and Liang E. Stiffness predictions for unidirectional short-fiber composites: review and evaluation. Composites Science and Technology 1999;59:655-671.
2. Lusti HR, Hine PJ and Gusev AA. Direct numerical predictions for the elastic and thermoelastic properties of short fibre composites. Composites Science and Technology 2002;62:1927-1934.
3. Friedrich K. Microstructural efficiency and fracture toughness of short fiber/thermoplastic matrix composites. Composites Science and Technology 1985;22:43-75.
4. Whiteside BR, Simulation and validation of fibre orientation in injection mouldings. 2001, University of Bradford.
5. Clarke AR, Davidson N and Archenhold G, *Mesostructural characterisation of aligned fibre composites*, in *Flow induced alignement in composite materials*, T.D. Papathanasiou and D.C. Guell, Editors. 1997, Woodhead Publishing.
6. Hine PJ, Davidson N, Duckett RA, Clarke AR and Ward IM. Hydrostatically extruded glass-fiber-reinforced polyoxymethylene. I: The development of fiber and matrix orientation. Polymer Composites 1996;17:720-729.
7. O'Connell PA and Duckett RA. *Fibre orientation and impact behaviour of injection moulded samples of short fibre reinforced carbon fibre/PEEK composites*. in *Fibre Reinforced Composites 98*. 1988. Liverpool: Plastics and Rubber Institute.
8. Williams JG and Cawood MJ. European Group on Fracture - Kc and Gc Methods for Polymers. Polymer Testing 1990;9:15-26.
9. Advani SG and Tucker III CL. The use of tensors to describe and predict fibre orientation in short fibre reinforced composites. Journal of Rheology 1987;31:751-784.
10. Kelly A and Tyson WR, in *High Strength Materials*, V.F.Zackey, Editor. 1965, Wiley: New York.